

A nucleate boiling limitation model for the prediction of pool boiling CHF

Heung June Chung^{a,*}, Hee Cheon No^b

^a *Thermal Hydraulic Safety Research Department, Korea Atomic Energy Research Institute, P.O. Box 105, Yuseong, Daejeon 305-600, Republic of Korea*

^b *Department of Nuclear and Quantum Engineering, Korea Advanced Institute of Science and Technology, 373-1 Kusong-dong, Yuseong, Daejeon 305-701, Republic of Korea*

Received 15 May 2006; received in revised form 14 December 2006
Available online 26 March 2007

Abstract

A nucleate boiling limitation model which is applicable to the heat transfer prediction in the nucleate boiling region and the CHF was proposed for a pool boiling. The present model was developed based on the direct observations of the physical boiling phenomena. The predicted boiling curves for the nucleate boiling region agree well with both the vertical and the horizontal surface data for all the contact angles. The predicted CHF for the vertical surface also agrees well with the experimental data, but the present model underpredicts the CHF by about 30% for the horizontal surface data.

© 2007 Elsevier Ltd. All rights reserved.

Keywords: Active nucleation site density; Dry area fraction; Nucleate boiling limitation model

1. Introduction

The accurate prediction of the boiling characteristic curve including a critical heat flux (CHF) is essential for the design and safe operation of high power density thermal systems such as boilers, heat exchangers, and nuclear reactors. Consequently, a plethora of empirical correlations and theoretical models on a pool and flow boiling have been presented in these engineering fields. However, a number of the current CHF models were formulated based on the postulation of a CHF mechanism without an observation of the physical boiling phenomena. This is mainly due to the fact that an observation of the boiling phenomena near the heater surface is very difficult. Also, as several investigators have suggested [1,2], a realistic CHF model would be one that has a natural outcome of

a description of the high-heat flux nucleate boiling region in contrast to the traditional view of a CHF as an independent phenomenon distinct from a nucleate boiling.

Dhir and Liaw [3] predicted a CHF and transition boiling heat fluxes under the assumption of the existence of stationary vapor stems. This model seems to be successful in predicting a CHF at a variety of contact angles. However, as Sadasivan et al. [1] indicated, this model is not realistic because vapor stems associated with individual active nucleation sites are not distributed over the surface in a regular manner.

Ha and No [2], Kolev [4], and Zhao et al. [5] presented theoretical models that take into consideration an individual bubble behavior. Ha and No [2] presented a dry spot model which can predict the CHF for a pool and a flow boiling. They postulated that when the nucleating bubbles in a cell exceed a critical number, the liquid supply into the cell is stopped and dry spots occur. Then, the dry spots coalesce with each other and a CHF occurs. However, the dry spot formation mechanism in their model is not consistent with the experimental observations by Chung

* Corresponding author. Tel.: +82 42 868 2077; fax: +82 42 868 8362.
E-mail address: hjchung@kaeri.re.kr (H.J. Chung).

Nomenclature

A	cell area [m^2]
A_{dry}	dry area [m^2]
CHF	critical heat flux [W/m^2]
N	local active nucleation site density in a given area A [sites/ m^2]
\bar{N}	average density of active sites in a heating surface [sites/ m^2]
n	number of bubbles
n_A	number of bubbles without coalescence
n_{ib}	number of bubbles without coalescence in a given area A
NBF	nucleate boiling fraction
P	probability function
q	heat flux [W/m^2]
q_b	heat transferred by a single bubble site [W/site]
q_{NB}	nucleate boiling heat flux [W/m^2]
T	temperature [K]
ΔT_{ws}	wall superheat [K]

Greek symbols

ϕ	contact angle [deg]
Φ_{NB}	nucleate boiling fraction
$\Gamma_{\text{dry,c}}$	dry area fraction occupied by the coalesced dry areas
$\Gamma_{\text{dry,i}}$	dry area fraction occupied by the isolated dry spots
$\Gamma_{\text{dry},\phi}$	dry area fraction with contact angle of ϕ
$\Gamma_{\text{dry,ref}}$	reference dry area fraction

Subscripts

m	measured
p	predicted
ref	reference value

and No [6]. Kolev [4] considered the fluctuation frequency as a function of the bubble departure frequency. This model shows a good agreement with the experimental data. But, some empirical constants are introduced into the model to match the prediction to the experimental data. Zhao et al. [5] formulated a microlayer model by considering the behaviors of individual bubbles beneath a vapor mushroom. Even though their final prediction equation is somewhat complicated, the prediction results show a fairly good agreement with the experimental data.

Recently, Buhholz et al. [7], Lüttich et al. [8], and Auracher and Marquardt [9] presented valuable results for entire boiling curves. Auracher and Marquardt conducted pool boiling experiments for well-wetting fluids and fluids with a large contact angle. Based on the experimental results, they made single and reproducible boiling curves. Also, they proposed an interfacial area density model which is being developed and recommended that the interfacial area density be measured by using a special 4-tip probe. In their paper, evaporation around the contact lines is the governing mechanism along the entire boiling curve. For a measurement of that quantity, Euh et al.'s results can be used as a reference methodology [10]. They developed a five sensor conductivity probe and formulated a mathematical approach for measuring the interfacial area concentration.

As discussed above, a realistic CHF model would be one that incorporates the directly observed CHF mechanism rather than any postulations. In the present study, based on the results of the direct observations of the physical boiling phenomena near a CHF, a nucleate boiling limitation model which can predict a heat transfer in a nucleate boiling region including a CHF is proposed for a pool boiling. Verification of the performance of the prediction is

accomplished by a comparison with the existing experimental data.

2. Observation of CHF mechanism

As described in the previous section, Chung and No [6] presented a directly observed CHF mechanism for a pool boiling of R-113 on a horizontal surface. In their experiment, a CHF was defined as the highest heat flux that the heater surface temperature was maintained as stable before a temperature excursion commenced by a slight increase in the heat flux. At a CHF, most of the heater surface becomes dry and the liquid–solid contact fraction decreases to below 30% and the wetted pattern is not a continuous plane type but maze-like curves. Also, at a CHF, a large vapor film covers a large part of the heater surface, and an intense nucleate boiling takes place around the edge of a large vapor film. Some nucleating bubbles in this locally-wetted region coalesce laterally and form another small vapor film. This small vapor film does not become large, and a wetting region is formed repeatedly.

A large vapor film, which covers a large part of the heater surface, collapses when its upper interface departs. After the large vapor film collapses, a short wetting occurs. If the surface is intermittently wetted, a vigorous boiling occurs and a continuous vapor film resulting from a coalescence of the vapor bubbles is reestablished. Vapor stems and a dryout of the macrolayer was not observed. Instead of vapor stems and a dryout of the macrolayer, a local nucleate boiling occurs under the large vapor film and at the edge of it. From the above observations, it is noted that a nucleate boiling takes place around the edge of a large vapor film and underneath a departing large vapor mass. This means that, even though the vapor film covers a large

fraction of the heater surface, the local nucleate boiling in the wetted region plays a key role in determining whether the heater surface temperature increases further or not.

At a CHF, a slight increase of the heat flux causes the commencement of a temperature excursion. This situation, just after a CHF, is called a CHF(+). At a CHF(+), only a brief nucleate boiling occurs at the edge of a vapor film. However, the wetted region quickly becomes a dry region with a continuous vapor film and then the nucleate boiling is limited by an agglomeration of the nucleating bubbles. As a result of this limited nucleating boiling activity at the local wetted part of the heater surface, the heater surface temperature begins to increase further, resulting in a burnout. These observations are similar to the reduced boiling activity by Galloway and Mudawar [11] and Celata et al. [12]. Consequently, it can be concluded that a CHF comes from the locally-limited nucleate boiling activity rather than any changes of the hydrodynamic conditions.

3. A nucleate boiling limitation model

3.1. Concept of the nucleate boiling fraction

As discussed in the previous section, a nucleate boiling limitation in the wetted region governs both a CHF and a nucleate boiling heat transfer. In addition, Chung and No [6] experimentally investigated a dry spot formation mechanism and the role of a dry area under a large vapor mass. They found that an increased resident time of the large dry area in the local vapor film regime influences the heat transfer mechanism and, consequently, the slope of the boiling curve apparently changes. Isolated dry spots or short periods of dry areas from the coalesced bubbles hardly affected the boiling curve. Another important experimental observation is that the dry spots and the bubbles occur simultaneously. This means that, when a bubble nucleates and grows at an active nucleation site, a dry spot is formed below the corresponding bubble. Therefore, these should be considered as a synchronized identity rather than an independent one. Therefore, we can extract information about the number of bubbles from that of the dry spots.

Based on these experimental observations, the quantity of the heat transferred by all the bubbles in the region that the coalescence effects is not dominant can be represented as $q_b \bar{N}$, where q_b is the heat transferred by a single bubble site by assuming each bubble site has a uniform heat transfer capacity, and \bar{N} is the average density of the active nucleation sites. If we ignore the heat flux fractions due to a single-phase convection and a film boiling, $q_b \bar{N}$ can be presumed as a nucleate boiling heat flux, q_{NB} . The nucleate boiling heat flux curve can be estimated from a linear fitting of a nucleate boiling region as a function of the wall superheat as shown in Fig. 1. If there is no formation of a large dry area beyond the nucleate boiling region (Region II in boiling curve, Fig. 1), the heat flux increases along the curve q_{NB} with the surface superheat. However, as a large dry area occurs, the heat transfer deteriorates and

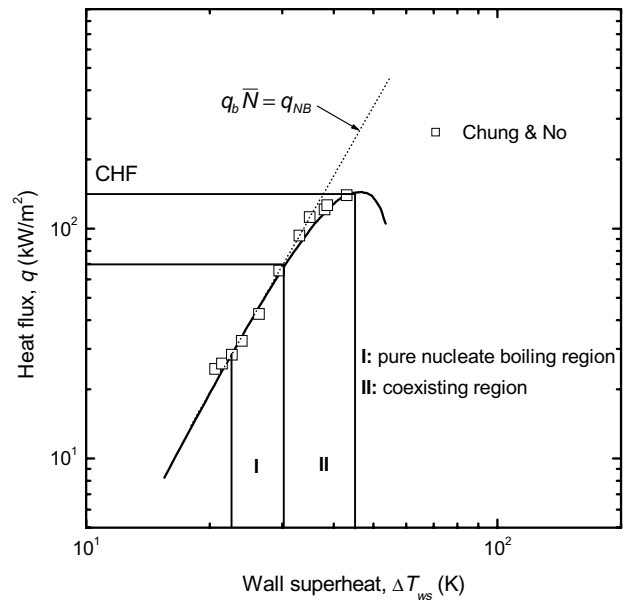


Fig. 1. Typical boiling curve.

the boiling curve deviates from the curve, q_{NB} . This is due to a decrease of the fraction of a pure nucleate boiling without a coalescence of the bubbles. Therefore, if we can obtain quantitative information on the pure nucleate boiling fraction in the coalesced boiling regime, we can evaluate the overall heat flux in region II under the assumptions that the heat flux fractions due to a single-phase convection and a film boiling are negligible. Consequently, the prediction of a quantitative nucleate boiling fraction in any boiling regime is essentially required to obtain the overall heat flux.

Now, let us apply the concept of a nucleate boiling fraction to the prediction of the R-113 pool boiling curve. To obtain the nucleate boiling fraction, first, the number of isolated bubbles without a coalescence, n_{ib} , in a given area, are counted from the behaviors of the dry spots observed by Chung and No [6]. And second, the active nucleation site density, ϕ , is given by using Wang and Dhir's correlation [13] as follows:

$$\bar{N} = 5 \times 10^{-27} (1 - \cos \phi) / d_c^6, \quad (1)$$

where ϕ and d_c are the contact angle and cavity mouth diameter in their model, respectively.

Then, we obtain the expected number of isolated bubbles in a given area A

$$n_A = \bar{N} \times A. \quad (2)$$

For the present analysis, a contact angle of 14° is used, because the experimentally obtained active nucleation site density agreed well with the case of 14° of Wang and Dhir's correlation as shown in Fig. 2. Then, the nucleate boiling fraction (NBF, Φ_{NB}) is defined as

$$\Phi_{NB} = n_{ib} / n_A, \quad (3)$$

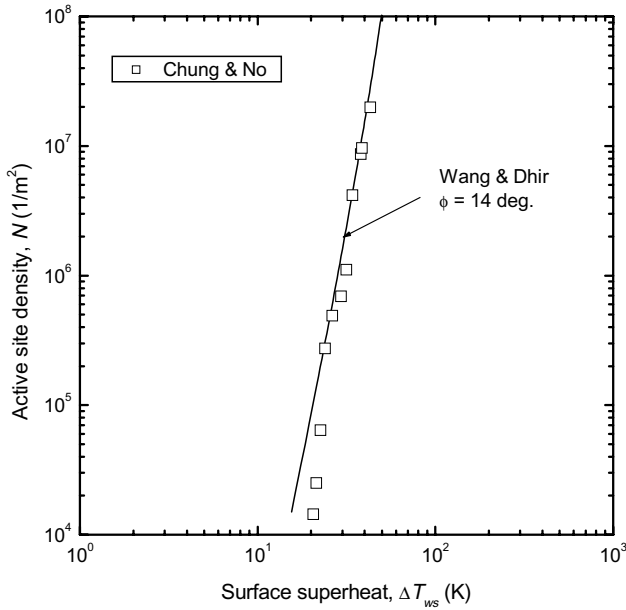


Fig. 2. Active site density for pool boiling of R-113.

where n_{ib} and n_A are the number of isolated bubbles without a coalescence and the expected number of isolated bubbles in a given area A , respectively. The physical meaning of the NBF is the ratio of the number of the isolated bubbles contributing to a pure nucleate boiling to the number of bubbles which may exist in a given area A . By using the above NBF, the overall heat flux from a nucleate boiling to a CHF can be represented as the following relation:

$$q = q_b \bar{N} \Phi_{NB} = q_{NB} \Phi_{NB} \quad (4)$$

A comparison of the prediction by using the concept of a NBF with the experimental data is shown in Fig. 3. As

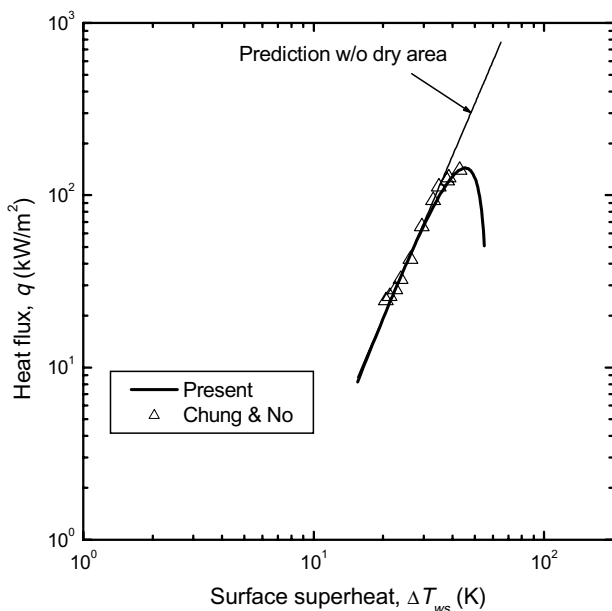


Fig. 3. Comparison of prediction with R-113 pool boiling data using concept of nucleate boiling fraction.

can be seen in this figure, the prediction has a good agreement with the measured data from the nucleate boiling regime to the CHF. This result indicates that the nucleate boiling fraction should be one of the important quantities representing the nucleate boiling heat flux from the nucleate boiling regime to the CHF.

3.2. Basic assumptions

To simplify the modeling for both a CHF and a nucleate boiling heat flux, the following are assumed:

- (1) The number density of the active nucleation sites increases as the wall heat flux or the superheat increases. Because addition of new active nucleation sites influences the rate of a heat transfer from a heater surface, its knowledge of the active nucleation site density and distribution is required in order to develop a credible model for the prediction of a nucleate boiling heat flux. As a first investigation of the distribution of active nucleation sites, Gaertner [14] found that active sites are randomly distributed on a heating surface and their spatial distribution obeys Poisson distribution. The Poisson distribution of an active nucleation site was confirmed by Sultan and Judd [15] and Kenning and Del Valle [16]. Thus, when an average active site density of \bar{N} is known for the whole heater surface area, and if it is divided into a number of small sub-areas A , then the area fraction where a local site density of N on a local heater surface area A can be calculated according to

$$P(NA) = \frac{e^{-\bar{N}A} (\bar{N}A)^{NA}}{(NA)!}, \quad (5)$$

where $P(NA)$ is the fraction of a sub-area in which active sites of NA are found, NA and $\bar{N}A$ the actual number and the expected number of active sites in sub-area A .

- (2) As is generally known, for a high-heat flux nucleate boiling up to a CHF, the heat flux fractions due to a pure natural convection and due to a pure film boiling are much smaller than that due to a pure nucleate boiling.

3.3. Proposed model

As discussed in the previous section, the nucleate boiling fraction (NBF) in a given boiling area defined as Eq. (3) is a key parameter for evaluating the heat flux contributing to nucleate boiling without a coalescence.

Let us consider an arbitrarily selected area A as shown in Fig. 4. In this selected area, some isolated nucleating bubbles and coalesced bubbles coexist. As discussed in the previous section, isolated nucleating bubbles and coalesced bubbles correspond to the isolated dry spots and the coalesced dry areas, respectively. Here, the coalesced

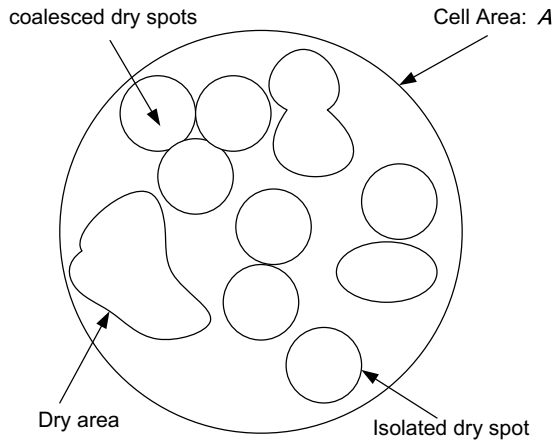


Fig. 4. Configuration of the conceptual dry area.

dry areas mean not only the coalesced dry spots but also the dry areas. In this situation, the probability of the existence of isolated dry spots without a coalescence is related to the NBF. As shown in Fig. 4, the total dry area is a summation of the dry areas occupied by all the isolated dry spots and the coalesced dry areas, and the dry area fraction is defined as

$$\Gamma_{\text{dry}} = A_{\text{dry}}/A. \quad (6)$$

Then, if there are some isolated dry spots and coalesced dry areas in the dry area, A_{dry} , the dry area fraction contains the sub-probabilities of the isolated dry spots and the dry areas. Thus we can take it as

$$P(\Gamma_{\text{dry},i}) + P(\Gamma_{\text{dry},c}) = 1, \quad (7)$$

and obtain

$$P(\Gamma_{\text{dry},i}) = 1 - P(\Gamma_{\text{dry},c}), \quad (8)$$

where $P(\Gamma_{\text{dry},i})$ is the probability of a dry area fraction or the sub-fraction occupied by the isolated dry spots and $P(\Gamma_{\text{dry},c})$ is the probability of a dry area fraction or the sub-fraction occupied by the coalesced dry areas.

Based on the assumption that the distribution of the active nucleation sites obeys the Poisson distribution, Hsu [17] studied the bubble populations of methanol and water on narrow heating strips and tabulated the percentage of the merging bubbles as a function of the heat flux and bubble size. By analyzing the experimental data, Hsu obtained the probability of a coalescence between bubbles in one cell in the following statistical relation:

$$P(Co) = 1 - e^{-\bar{N}A}(\bar{N}A + 1). \quad (9)$$

Using Eqs. (8) and (9) yields

$$P(\Gamma_{\text{dry},i}) = 1 - \Gamma_{\text{dry}} \times P(Co). \quad (10)$$

Eq. (10) means the fraction of the isolated bubbles without a coalescence in a given area A . Then, we can obtain the number of bubbles without a coalescence contributing to a pure nucleate boiling

$$n_{\text{ib}} = \bar{N} \times A \times P(\Gamma_{\text{dry},i}). \quad (11)$$

As described in Eq. (2), the number of bubbles expected in a given area A becomes

$$n_A = \bar{N} \times A. \quad (12)$$

Therefore, using Eqs. (11) and (12) we can obtain the nucleate boiling fraction, NBF, as follows:

$$\Phi_{\text{NB}} = n_{\text{ib}}/n_A = 1 - \Gamma_{\text{dry}} \times P(Co). \quad (13)$$

Subsequently, the heat flux contributing to a nucleate boiling is obtained as the following equation:

$$q = q_b \bar{N} \Phi_{\text{NB}}. \quad (14)$$

3.4. Prediction results and discussion

As a first step for a comparison, the reference dry area fraction for water, which is required to calculate the number of bubbles in a given boiling area, is obtained from a regression of the experimental data by Chung and No [6]. Because, the contact angle in their experiments is the case of a somewhat lower range of the contact angles (14°), the following regression equation as a function of the wall superheat is used:

$$\Gamma_{\text{dry,ref}} = 0.3631 - 0.0258\Delta T_{\text{ws}} + 9.4019 \times 10^{-4}\Delta T_{\text{ws}}^2. \quad (15)$$

The experimental data for the dry area fraction given in most literatures cover the transition boiling region beyond the nucleating boiling region [18–20]. Therefore, there is little available data especially on the partial nucleate boiling regime. In the present study, to take into account the contact angle effect on the dry area fraction, the analytical results by Ha and No [21] were used. With a reference contact angle based on the present experimental data and by considering the effect of a contact angle on the dry area fraction, the following equation is derived:

$$\Gamma_{\text{dry},\phi} = \Gamma_{\text{dry,ref}} \times F(\phi), \quad (16)$$

where

$$F(\phi) = 0.97 - 0.0038\phi + 3.68 \times 10^{-4}\phi^2, \quad (17)$$

where ϕ is a contact angle as degrees.

A comparison of the present model of Eq. (14) with the experimental data was accomplished by using Liaw and Dhir's results [22]. Liaw and Dhir conducted pool boiling experiments for saturated water at an atmospheric pressure on a vertical rectangular copper surface with several contact angles. Figs. 5–8 show the prediction results by using the water boiling data for several contact angles. It can be noted from these figures that the prediction results agree well with the data by Liaw and Dhir in the region of a nucleate boiling as well as a CHF for all the contact angles.

In Fig. 6, the present work was also compared with Auercher and Marquardt's water pool boiling data [9]. They conducted steady-state boiling tests for distilled water on a horizontal copper surface under an atmospheric pressure condition. For their copper–water combination, the contact angle was assumed to be 30° according to the data

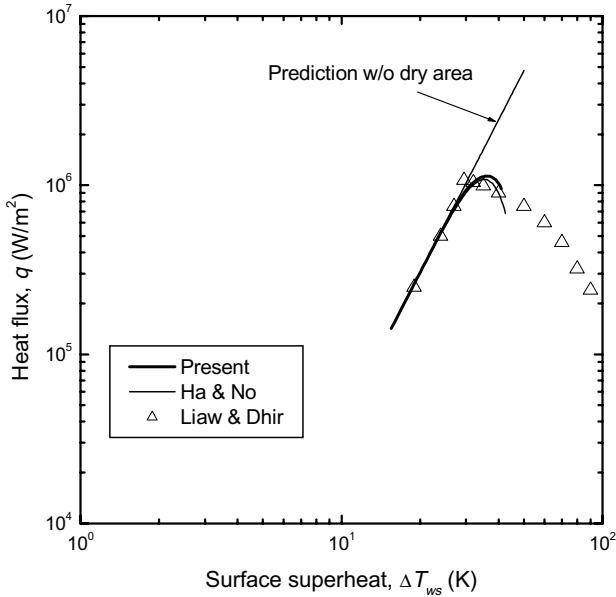


Fig. 5. Comparison of prediction with experimental data for contact angle of 14°.

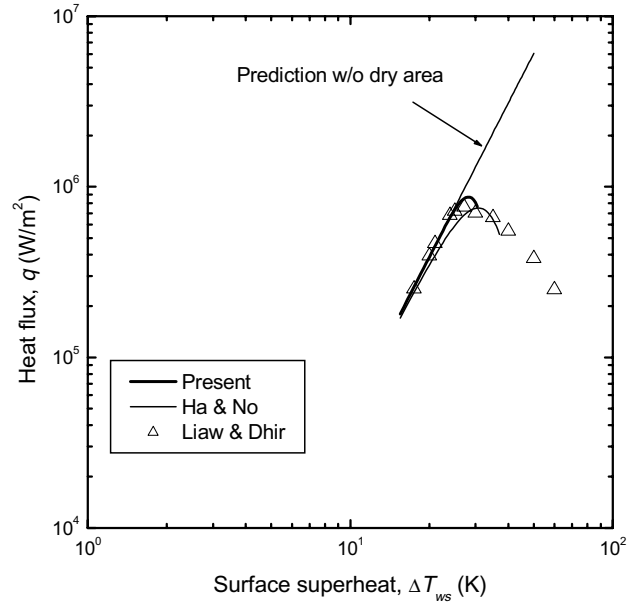


Fig. 7. Comparison of prediction with experimental data for contact angle of 38°.

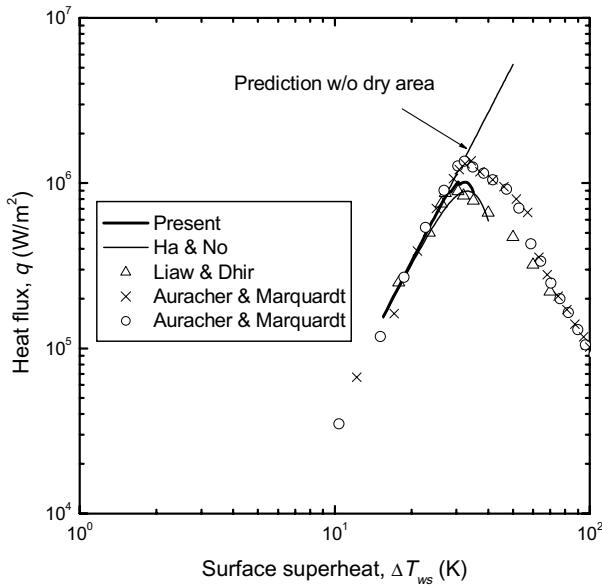


Fig. 6. Comparison of prediction with experimental data for contact angle of 27°.

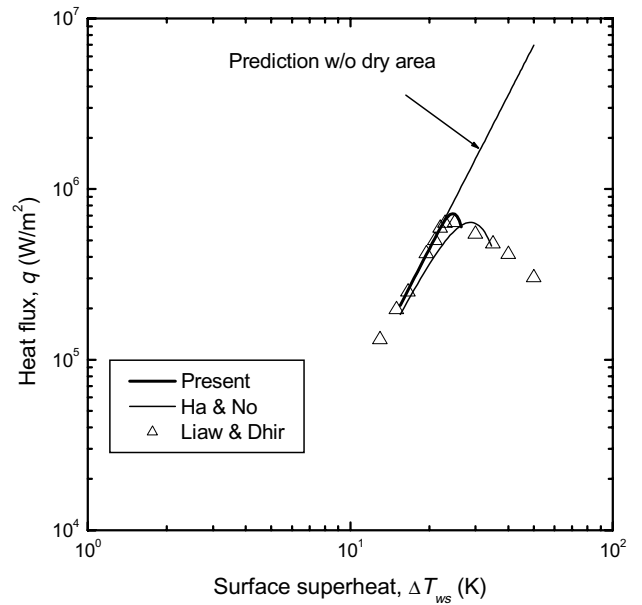


Fig. 8. Comparison of prediction with experimental data for contact angle of 69°.

by Basu et al. [23]. Therefore, their data are compared with the case for a contact angle of 27° of the present work. In Fig. 6, the present model underpredicts the CHF by about 30% when compared to the data by Auracher and Marquardt. However, the present model agrees well with their data in the nucleate boiling region. This reasonably supports the face that the concept of a nucleate boiling fraction described in Section 3.1 is reliable from the heat transfer point of view. The discrepancies between Auracher and Marquardt’s data and the present work may due to the surface orientation effect as presented by Howard and Mudawar [24]. They concluded that a single overall pool

boiling CHF model can not possibly account for orientation effects, but instead different models should be developed for different orientations.

The present model was compared to Paul and Abdel-Khalik’s water pool boiling data [25]. They conducted experiments on the pool boiling of saturated water at 1 atm with an electrically heated horizontal platinum wire. They measured the active active nucleation site density and the bubble departure diameter up to 70% of a CHF. The mean number density of the active active nucleation sites

per unit length and the average bubble departure diameter can be obtained from their results:

$$\bar{N} = 1.207 \times 10^{-3} q_{NB} + 15.74. \tag{18}$$

The contact angle for this analysis was assumed to be 38°, and the measured CHF was $0.72 \times 10^6 \text{ W/m}^2$ and the predicted value was $0.701 \times 10^6 \text{ W/m}^2$ as shown in Fig. 9.

In the present study, the prediction model was formulated based on the directly observed boiling phenomena in the vicinity of the heater surface with the measured active nucleation site and an analytical dry area fraction. However, some experimental correlations included in the present model may cause the discrepancies between the vertical and the horizontal CHF values. Therefore, we need to perform further work on a measurement for the active nucleation site density and the dry area fraction for vertical and horizontal surfaces, respectively. Based on these experimental results, more realistic and reliable models for the active nucleation site density and the dry area fraction which are applicable to vertical and horizontal surfaces should be developed.

To examine the sensitivity of a CHF to the main parameters, a sensitivity analysis was carried out. For the present model, the major parameters affecting a CHF are the dry area fraction and the active site density. With an intermediate variable X such as the dry area fraction and the active site density, the sensitivity S is defined as

$$S = \frac{\text{CHF}_m - \text{CHF}_p(X)}{\text{CHF}_m} \times 100\%. \tag{19}$$

Using Liaw and Dhir’s experimental data, the results of the sensitivity analysis are presented in Figs. 10 and 11. In these figures, $\Gamma_{dry,ref}$ and \bar{N}_{ref} are the values given by the closure value of the predicted CHF for the experimental data. As shown in Figs. 10 and 11, a 10% variation of

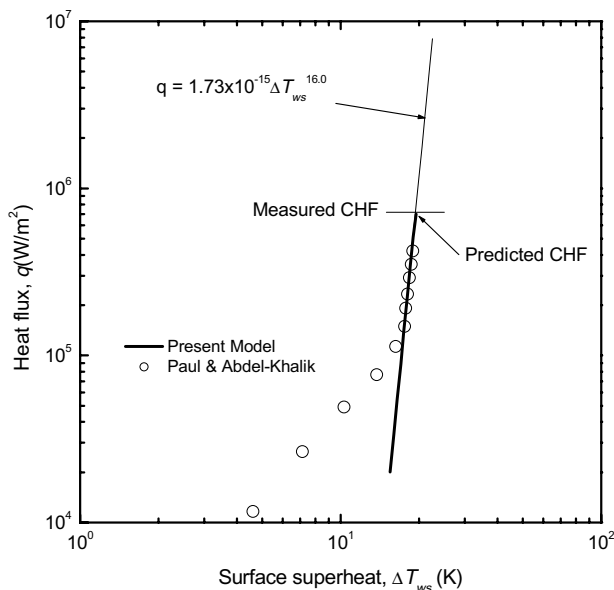


Fig. 9. Comparison of predictions with data for horizontal wire.

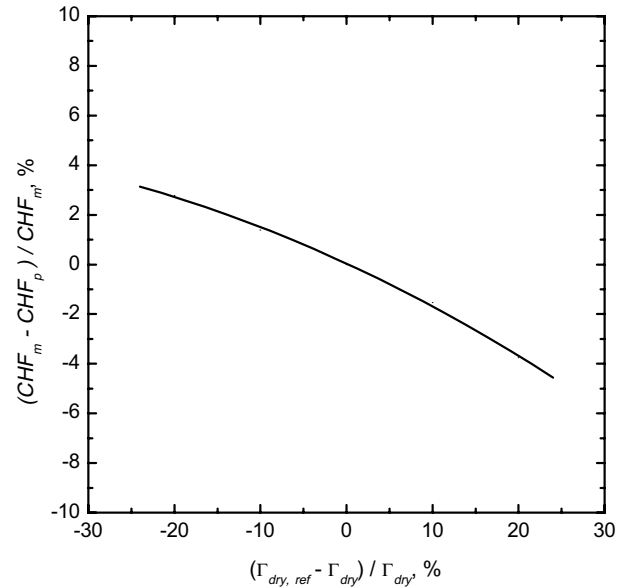


Fig. 10. The sensitivity of CHF with respect to the dry area fraction.

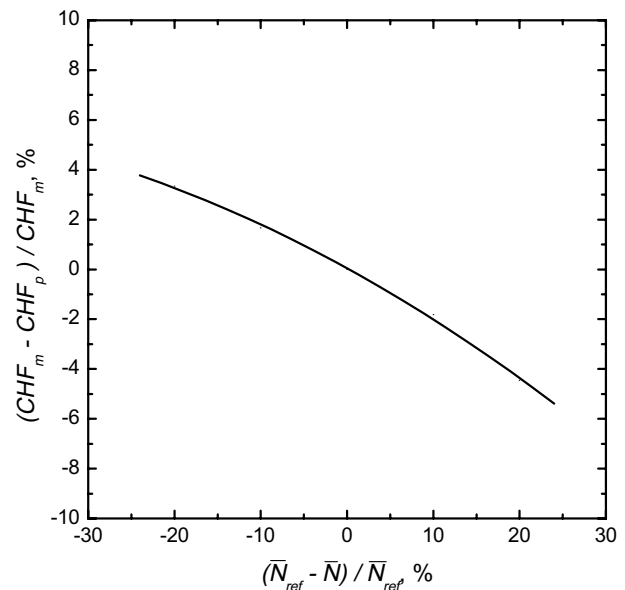


Fig. 11. The sensitivity of CHF with respect to the active site density.

the dry area fraction and the active site density results in a variation of a CHF to within 2%. From these sensitivity analyses, it is noted that the present model is very stable with respect to a variation of the major parameters such as the dry area fraction and the active nucleation site density.

4. Conclusions and recommendations

An approach in order to incorporate the direct observations of boiling phenomena into a heat transfer prediction formulation was made, and a nucleate boiling limitation model which is applicable to the prediction of a heat

transfer in a nucleate boiling region and of a CHF was proposed for a pool boiling. Verification of the performance of the proposed model was accomplished by a comparison with the existing experimental data, and the followings were derived:

- (1) The heat transfer prediction for the nucleate boiling region agrees well with both the vertical and horizontal surface data for all the contact angles. This means that the concept of a nucleate boiling fraction adopted in the present work is reliable from the heat transfer point of view.
- (2) The CHF prediction for the vertical surface also agrees well with the experimental data, but the present model underpredicts the CHF by about 30% when compared to the horizontal surface data. This discrepancy may due to the surface orientation effects on the CHF mechanism.

In the present study, a prediction model was formulated based on the directly observed boiling phenomena in the vicinity of a horizontal heater surface with the measured active nucleation site density and an analytical dry area fraction. However, the present model shows that the predicted CHF values for the vertical and the horizontal surfaces are discrepant. Therefore, we need to perform further work on the measurement for the active nucleation site density and the dry area fraction for the vertical or the horizontal surfaces, respectively. Based on these experimental results, more realistic and reliable models for the active site density and the dry area fraction which can be applicable to vertical and horizontal heating surfaces should be developed.

References

- [1] P. Sadasivan, C. Unal, R. Nelson, Perspective: issues in CHF modeling – the need for new experiments, *ASME J. Heat Transfer* 117 (1995) 558–567.
- [2] S.J. Ha, H.C. No, A dry-spot model of critical heat flux in pool and forced convection boiling, *Int. J. Heat Mass Transfer* 41 (2) (1988) 303–311.
- [3] V.K. Dhir, S.P. Liaw, Framework for a unified model for nucleate and transition pool boiling, *ASME J. Heat Transfer* 111 (1989) 739–746.
- [4] N.I. Kolev, How accurately can we predict nucleate boiling? *Exp. Therm. Fluid Sci.* 10 (1995) 370–378.
- [5] Y.H. Zaho et al., Unified theoretical prediction of fully developed nucleate boiling and critical heat flux based on a dynamic microlayer model, *Int. J. Heat Mass Transfer* 45 (2002) 3189–3197.
- [6] H.J. Chung, H.C. No, Simultaneous visualization of dry spots and bubbles for pool boiling of R-113 on a horizontal heater, *Int. J. Heat Mass Transfer* 46 (2003) 2239–2251.
- [7] M. Buchholz et al., Experimental investigation of local process in pool boiling along the entire boiling curve, in: *Proceedings of the Fifth International Conference on Boiling Heat Transfer*, Montego Bay, Jamaica, 2003.
- [8] T. Lüttich et al., Towards a unifying heat transfer correlation for the entire boiling curve, in: *Proceedings of the Fifth International Conference on Boiling Heat Transfer*, Montego Bay, Jamaica, 2003.
- [9] H. Auracher, W. Marquardt, Heat transfer characteristics and mechanisms along entire boiling curves under steady-state and transient conditions, *Int. J. Heat Fluid Flow* 25 (2004) 223–242.
- [10] D.J. Euh et al., Development of the interfacial area concentration measurement method using a five sensor conductivity probe, *J. Korean Nucl. Soc.* 32 (5) (2000) 433–445.
- [11] J.E. Galloway, I. Mudawar, CHF mechanism in flow boiling from a short heated wall-I. Examination of near-wall conditions with the aid of photomicrography and high-speed video imaging, *Int. J. Heat Mass Transfer* 30 (10) (1993) 2511–2526.
- [12] G.P. Celata et al., Visual investigation of high heat flux burnout in subcooled flow boiling of water, in: *Third International Conference on Multiphase Flow, ICMF'98*, Lyon, France, 1998.
- [13] C.H. Wang, V.K. Dhir, Effect of surface wettability on active nucleation site density during pool boiling of water on a vertical surface, *ASME J. Heat Transfer* 115 (1993) 659–669.
- [14] R.F. Gaertner, Distribution of active sites in the nucleate boiling of liquids, *Chem. Eng. Prog. Symp. Ser.* 59 (41) (1963) 52–61.
- [15] Sultan, M. Judd Sultan, R.L. Judd, Spatial distribution of active sites and bubble flux density, *Trans. ASME J. Heat Transfer* 100 (1978) 56–62.
- [16] D.R.B. Kenning, M.V.K. Del Valle, Fully-developed nucleate boiling: overlap of areas of influence and interference between bubble sites, *Int. J. Heat Mass Transfer* 24 (6) (1981) 1025–1032.
- [17] Y.Y. Hsu, R.W. Graham, *Transport Processes in Boiling and Two-Phase Systems*, McGraw-Hill, New York, 1976, pp. 39–49.
- [18] A.A. Alem Rajabi, R.H.S. Winterton, Liquid–solid contact in steady-state transition pool boiling, *Int. J. Heat Fluid Flow* 9 (2) (1988) 215–219.
- [19] D.S. Dhuga, R.H.S. Winterton, Measurements of surface contact in transition, *Int. J. Heat Mass Transfer* 28 (10) (1985) 1869–1880.
- [20] H.S. Ragheb, S.C. Cheng, Surface wetted area during transition boiling in forced convective flow, *ASME J. Heat Transfer* 101 (1979) 381–383.
- [21] S.J. Ha, H.C. No, A dry-spot model for transition boiling heat transfer in pool boiling, *Int. J. Heat Mass Transfer* 41 (1998) 3771–3779.
- [22] S.P. Liaw, V.K. Dhir, Void fraction measurements during saturated pool boiling of water on partially wetted vertical surfaces, *ASME J. Heat Transfer* 111 (1989) 731–738.
- [23] N. Basu et al., Onset of nucleate boiling and active nucleation site density during subcooled flow boiling, *ASME J. Heat Transfer* 124 (2002) 717–728.
- [24] A.H. Howard, I. Mudawar, Orientation effects on pool boiling critical heat flux (CHF) and modeling of CHF for near vertical surfaces, *Int. J. Heat Mass Transfer* 42 (1999) 1665–1688.
- [25] D.D. Paul, S.I. Adel-Khalik, A statistical analysis of saturated nucleate boiling along a heated wire, *Int. J. Heat Mass Transfer* 26 (4) (1983) 509–519.